

# International Conference on Space Optics—ICSO 2022

Dubrovnik, Croatia

3–7 October 2022

*Edited by Kyriaki Minoglou, Nikos Karafolas, and Bruno Cugny,*



## *Pump Tunable Mirrorless OPO: an Innovative Concept for Future Space IPDA Emitters*



## Pump Tunable Mirrorless OPO: an Innovative Concept for Future Space IPDA Emitters

Kjell Martin Mølster<sup>a</sup>, Marie Guionie<sup>b</sup>, Patrick Mutter<sup>a</sup>, Jean-Baptiste Dherbecourt<sup>\*b</sup>, Jean-Michel Melkonian<sup>b</sup>, Xavier Delen<sup>c</sup>, Andrius Zukauskas<sup>a</sup>, Carlota Canalias<sup>a</sup>, Fredrik Laurell<sup>a</sup>, Patrick Georges<sup>c</sup>, Myriam Raybaut<sup>b</sup>, Antoine Godard<sup>b</sup>, and Valdas Pasiskevicius<sup>a</sup>

<sup>a</sup>Department of Applied Physics, Royal Institute of Technology (KTH), Roslagstullsbacken 21, Stockholm 10691, Sweden; <sup>b</sup>DPHY, ONERA, Université Paris-Saclay, F-91123 Palaiseau, France; <sup>c</sup>Université Paris-Saclay, Institut d'Optique Graduate School, CNRS, Laboratoire Charles Fabry, 91127, Palaiseau, France

\*jean-baptiste.dherbecourt@onera.fr

### ABSTRACT

A highly efficient mirrorless OPO tunable in the mid-infrared around 2  $\mu\text{m}$  has been developed and characterized in an original pumping configuration comprising a tunable high power hybrid Ytterbium laser MOPA (Master Oscillator Power Amplifier) in the nanosecond regime. The hybrid pump laser is based on a fiber laser seeder continuously tunable over several GHz at 1030 nm, which is shaped in the time domain with acousto-optic modulators (AOM), and power amplified in a dual stage Ytterbium doped fiber amplifiers, followed by two Yb:YAG bulk amplifiers. The pump delivers up to 3.5 mJ of energy within narrowband 15 ns pulses with a 5 kHz repetition rate. The output was focused into Periodically Poled KTP (PPKTP) crystals with a quasi-Phase Matching (QPM) period of 580 nm, producing Backward Optical Parametric Oscillation (BWOPO), with a forward signal wave at 1981 nm and a backward traveling idler at 2145 nm. We report significant optical to optical efficiencies exceeding 70 % depending on crystal length and input power. As theoretically expected, the forward wave could be continuously tuned over 10 GHz following the pump frequency sweep, while the backward wave remains almost stable, both being free from mode hops. These properties obtained from an optical arrangement without free-space cavities are attractive for future space Integrated Path Differential Absorption (IPDA) Lidar applications, which require robust and efficient tunable frequency converters in the mid-infrared.

**Keywords:** Hybrid laser, Master Oscillator Power Amplifier (MOPA), single frequency infrared laser sources, Backward Optical Parametric Oscillator (BWOPO), Integrated Path Differential Absorption Lidar (IPDA)

### 1. INTRODUCTION

In the frame of laser source development for spaceborne atmosphere remote sensing applications, parametric frequency down-converters and amplifiers offer the attractive prospects of high output power and wavelength tunability well into the mid-infrared. In the particular case of greenhouse gas measurements from space with the IPDA method, the main wavelength ranges of interest are located around 1.6  $\mu\text{m}$ , 2  $\mu\text{m}$ , and 3.9  $\mu\text{m}$ , where CH<sub>4</sub>, CO<sub>2</sub>, and N<sub>2</sub>O displays well-suited absorption lines<sup>1</sup>. These spectral windows can be reached with well characterized and mature pump laser sources<sup>2</sup> in combination with readily available nonlinear crystal materials well adapted for high fluence infrared generation and space applications such as LN, KTP, or KTA<sup>3-6</sup>. However, despite the improvement in gas concentration measurement capability and accuracy expected from a spaceborne IPDA Lidar<sup>7,8</sup>, core missions based on this method such as the German-French MERLIN (Methane Remote Sensing Lidar Mission)<sup>9</sup>, are scarce. This is partly due to the technical challenges to be overcome for a free-space high power parametric source to meet the optical, thermo-mechanical, and lifetime requirements imposed by the measurement principle and the operational environment for the instrument<sup>10-13</sup>. More specifically, critical characteristics such as beam propagation quality, pointing stability, and emitted wavelength tunability and accuracy, are directly related to the optical geometry and the alignment tolerances of the different components, which generally leads to rather complex designs, assembly, and control protocols, especially when multiple resonators are involved<sup>11,14-17</sup>. In the present study, we introduce an original “mirrorless” (i.e. without free-space cavity) pump and parametric source configuration, which may simplify future space IPDA emitters design, assembly, and

control. It is based on Backward-Wave Optical Parametric Oscillation (BWOPO) in combination with a tunable pump laser. The pump laser source is an Ytterbium based hybrid Master Oscillator Power Amplifier (MOPA), built on a sequence of fiber and free-space bulk amplification stages<sup>18</sup>. Preliminary experimental characterizations realized with 3.5 mJ and 15 ns pump pulses show promising output performances with infrared conversion efficiencies in the 50 % - 70 % range, and narrowband optical frequency tunability over several GHz, which motivates further research work for the use of this type of source either directly for remote gas sensing experiments, or as a tunable seeder for higher energy parametric amplification.

## 2. MIRRORLESS OPO PRINCIPLE AND PROPERTIES

### 2.1 Background

The BWOPO, initially proposed by Harris<sup>19</sup> in 1966, relies on the interaction of counter-propagating parametric waves in a  $\chi^{(2)}$  nonlinear crystal where the feedback required for oscillation build-up is distributed along the crystal itself as opposed to usual OPOs with co-propagating parametric waves where a resonant cavity provides an external feedback. The concept comes with the attractive prospect of avoiding the drawbacks generally associated with conventional OPOs such as the necessity of multi-wavelengths mirrors coatings subject to optical damage when intracavity power increases, resonant cavity(ies) alignments, or a limited miniaturization potential<sup>20</sup>. The key condition to realizing BWOPO is to compensate for the very large phase mismatch of counter-propagating signal and idler waves  $\Delta\mathbf{k} = \mathbf{k}_p - \mathbf{k}_f + \mathbf{k}_b$ , where  $\mathbf{k}_p$ ,  $\mathbf{k}_f$ , and  $\mathbf{k}_b$  stand for the pump, forward, and backward wave vectors. The first proposal considered birefringence phase matching, applicable in principle for an idler wavelength deep in the far infrared. With the advent of quasi-phase matching (QPM) nonlinear crystals in the 90's, BWOPO closer to degeneracy was considered again, and oscillation threshold intensity estimations showed typical values in the 100 MW/cm<sup>2</sup> range accessible with available pump lasers technologies<sup>21</sup>. However, in BWOPO the required QPM orientation period must be very small in the order of  $\lambda_{\text{pump}}/2$ , that is to say roughly 500 nm for conventional 1  $\mu\text{m}$  pump lasers, which is significantly more challenging to achieve than the QPM period for usual co-propagating OPO, typically ranging in the several tens of  $\lambda_{\text{pump}}$  (10  $\mu\text{m}$  -100  $\mu\text{m}$  for  $\lambda_{\text{pump}} = 1 \mu\text{m}$ ). The first successful BWOPO experimental demonstration was realized in 2007, within a periodically poled KTP (PPKTP) crystal, and a grating period of 800 nm<sup>22</sup>. In this pioneering work, two specific spectral properties of BWOPO could also be verified: *i*) pump wavelength tuning essentially affects the co-propagating beam wavelength while the counterpropagating beam wavelength remains almost fixed, and *ii*) the pump spectrum is essentially imprinted on the forward travelling wave while the backward wave linewidth is significantly narrower (two orders of magnitude narrower in<sup>22</sup>). Since this first demonstration, most of the experimental work has been carried out with sub-ns pulses in order to reach very high threshold intensities while avoiding optical damaging. Recent progresses on sub- $\mu\text{m}$  QPM structures fabrication in PPKTP have allowed for BWOPO pumping with 10 ns Q-switched pulses from an injection seeded Nd:YAG pump laser<sup>23</sup>, which further opens the path toward remote gas sensing applications. The present study follows this path by employing a tunable single frequency laser as the pump for a similar BWOPO device as in<sup>23</sup>.

### 2.2 BWOPO phase matching and tuning

The geometry and QPM configuration of the BWOPO studied in this paper is shown in Figure 1.

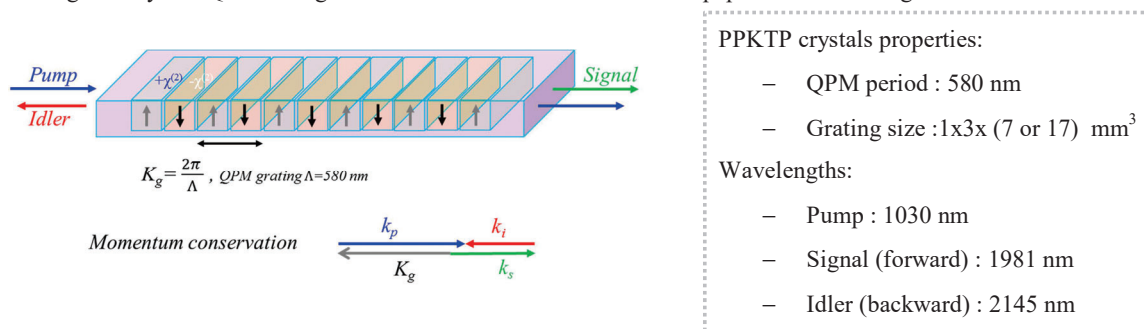


Figure 1: Schematic principle of the BWOPO in a periodically poled nonlinear crystal. The first order QPM condition with a 580 nm grating period and a 1030 nm pump wavelength result in a forward signal wave around 1981 nm.

The wavelength tuning of forward and backward waves can be achieved by modifying the quasi-phase matching condition  $\mathbf{k}_f + \mathbf{K}_g = \mathbf{k}_p + \mathbf{k}_b$ . In BWOP, this could be achieved by changing the QPM grating period either through mechanical translation to switch from one crystal grating to another or through crystal rotation for angular tuning as in<sup>24</sup>. Conversely to conventional co-propagating OPOs, temperature tuning is a very weak lever as it is inversely proportional to the sum of forward and backward refractive index instead of the difference, which result in a temperature tuning rate several orders of magnitude smaller for the BWOP<sup>22</sup>. As a consequence direct pump tuning is a very attractive feature in the perspective of gas remote sensing applications since it may provide fast tuning functionalities to probe the targeted molecules absorption features, without misalignment disadvantages.

Table 1. BWOP tuning rates with respect to pump wavelength tuning, calculated by first-order expansion of the phase matching condition.  $\omega_{p,f,b}$  and  $v_{p,f,b}$  designate the angular frequencies and group velocities for the pump, forward, and backward waves, respectively.

Forward wave tuning:	Backward wave tuning:
$\frac{\partial \omega_f}{\partial \omega_p} = \frac{v_{gf}(v_{gb} + v_{gp})}{v_{gp}(v_{gb} + v_{gf})} = 1 + \epsilon \quad (1)$	$\frac{\partial \omega_b}{\partial \omega_p} = \frac{v_{gb}(v_{gp} - v_{gf})}{v_{gp}(v_{gb} + v_{gf})} = -\epsilon \quad (2)$

As illustrated in Table 1 the specific phase matching condition in BWOP results in very different tuning rate of the forward and backward waves with respect to that of the pump. For the forward wave (signal wave in our case) the tuning rate is almost equal to 1, while the backward wave tuning rate is close to zero, meaning that pump wavelength variation are almost entirely imprinted on the forward wave.

### 2.3 Threshold and efficiency

Since there is no feedback assistance from a cavity resonator, one experimental challenge is to reach BWOP threshold with pump intensities significantly smaller than the optical damage threshold at the crystal interfaces. The theoretical expression for the BWOP threshold intensity in CW regime (assuming plane wave interaction) is given by the following expression<sup>25</sup>:

$$I_{th}^{CW} = \frac{\epsilon_0 c n_p n_f n_b \lambda_f \lambda_b}{32 d_{eff}^2 L^2} \quad (3)$$

Where  $\epsilon_0$  is vacuum permittivity,  $c$  the speed of light,  $d_{eff}$  the effective nonlinear coefficient of the crystal,  $L$  the grating length,  $n_{p,f,b}$  the refractive indices of pump, forward and backward waves, and  $\lambda_{f,b}$  the forward and backward wavelengths. With the parameters from Figure 1, the CW threshold intensity corresponding to the experimental cases exposed in part 3 are approximately **85 MW/cm<sup>2</sup>** and **15 MW/cm<sup>2</sup>** for the 7 mm and 17 mm PPKTP crystal, respectively, assuming a nonlinear coefficient of  $d_{eff} = 7$  pm/V. As illustrated by these numbers, the fabrication of long nonlinear crystals with a homogenous grating periodicity, which is highly challenging for sub- $\mu$ m periods, is the key to achieving a BWOP configuration with manageable pump intensities.

In the pulsed regime, the oscillation threshold peak intensity is higher than the CW theoretical threshold due to the parametric oscillation build-up time. This is all the more pronounced when the pump pulse duration is short i.e. comparable to the pump travelling time in the nonlinear crystal  $\tau = L/v_g$  (with  $v_g$  the pump group velocity, and  $L$  the crystal length). However, for pulse durations significantly longer than this travelling time, the CW calculation gives a valid order of magnitude of the threshold intensity. This is for example the case in reference<sup>23</sup>, where the nonlinear travelling time is approximately 44 ps (with a 7 mm long PPKTP), and the pump pulse duration 13 ns. This is also the case in our present experimental configuration where the travelling time are 44 ps and 106 ps (7 mm and 17 mm length PPKTP respectively) and the pump pulse duration is 15 ns. As illustrated later in part 3.2, the experimental threshold intensities were estimated to be **~100 MW/cm<sup>2</sup>** and **~20 MW/cm<sup>2</sup>**, in line with the estimation from equation (3). We refer the readers to the theoretical study published in<sup>25</sup> for a full detailed and complete description of BWOP in pulsed regime, where analytical formulas are derived to take into account the OPO build-up time influence on threshold and conversion efficiency.

One other attractive aspect of BWOP is that the parametric conversion efficiency presents a monotonic growth without the occurrence of the detrimental back conversion effects that are observed in co-propagating OPO for high pumping intensities. This relates to the fact that counter propagating signal and idler waves impose maximum intensities for both

waves to be reached at the opposite ends of the nonlinear crystal<sup>21,25</sup>. In CW plane wave approximation theory, the conversion efficiency can even get close to 100 % provided sufficient pump intensity. In practical experiments, although the conversion efficiency is reduced because of transverse phase and intensity inhomogeneity plus OPO build-up time, high conversion efficiencies superior to 50 % as well as high energy extraction > 1 mJ in both signal and idler beams have been demonstrated in the nanosecond regime<sup>23</sup>.

### 3. EXPERIMENTAL SET-UP

#### 3.1 Pump laser

In order to pump and tune the BWOP into the mid-infrared, we used a high power frequency agile Ytterbium MOPA that has been previously developed for tunable OPA experiments<sup>18</sup>. This laser source consists in a hybrid combination of fiber & bulk amplifiers respectively pumped at 976 nm and 940 nm. The general MOPA properties are summarized in the Figure 2 below. This configuration enables to produce a high power laser beam (3.5 mJ, 15 ns pulses at 5 kHz), with a very good beam quality ( $M^2 < 1.2$ ), while directly benefiting from the spectral agility of the CW seed laser with a continuous 10 GHz fast frequency tuning through piezoelectric modulation. These properties are well in line with the requirements to reach the BWOPs oscillation threshold, and to produce a narrowband tunable forward signal wave. As illustrated in Figure 2, this pump laser is currently a laboratory experimental bench, and characteristics such as pulse duration could be adjusted for future parametric studies.

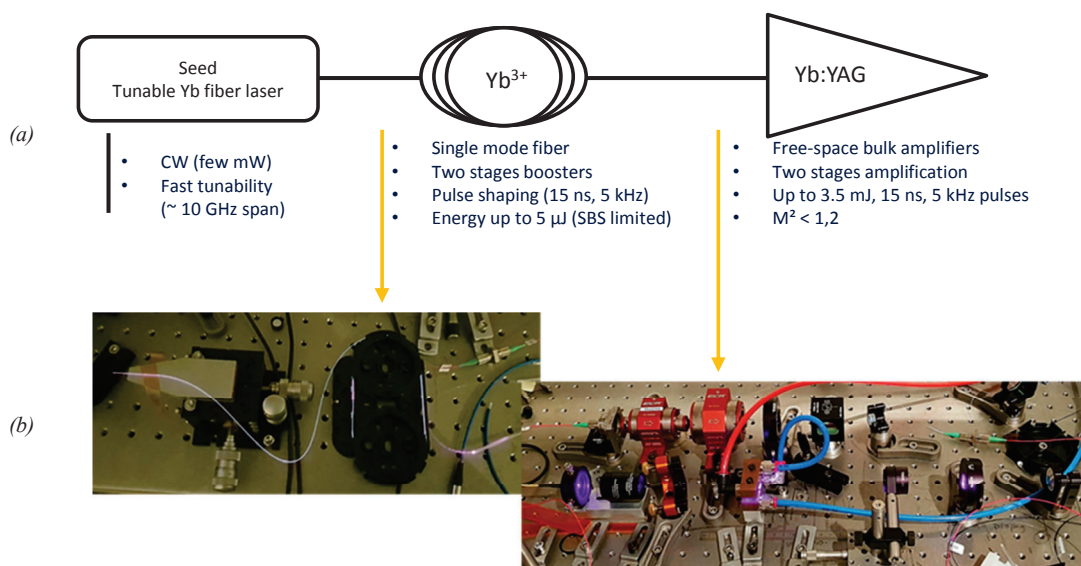


Figure 2: General architecture and characteristics of the Ytterbium MOPA pump laser (a), and overview of the experimental implementation of a fiber amplification stage and a bulk amplifier stage (b). We refer the reader to paper<sup>18</sup> for a detailed description and characterization of the set-up. SBS stands for Stimulated Brillouin Scattering.

#### 3.2 BWOP characterization

The pump laser beam is shaped in order to reach the hundreds of MW/cm<sup>2</sup> required to reach and exceed the BWOP oscillation threshold. It was focused on 140 μm radius (1/e<sup>2</sup>). Two PPKTP crystals of 7 mm and 17 mm length, with a 580 nm poling period were tested. The crystals are placed on a thermalized plate stabilized at slightly above ambient temperature at 27°C. The generated 1981 nm forward wave and the 2145 nm backward wave were separated from the pump beam with dichroic mirrors and characterized in power and central wavelength (Figure 3). All three beams were characterized with high finesse wavemeters; the pump beam with a WSU 10 ultimate, the forward wave with a WS/6 IR2, and the backward wave with a WS/6 IR3, all with frequency resolutions better than 100 MHz.

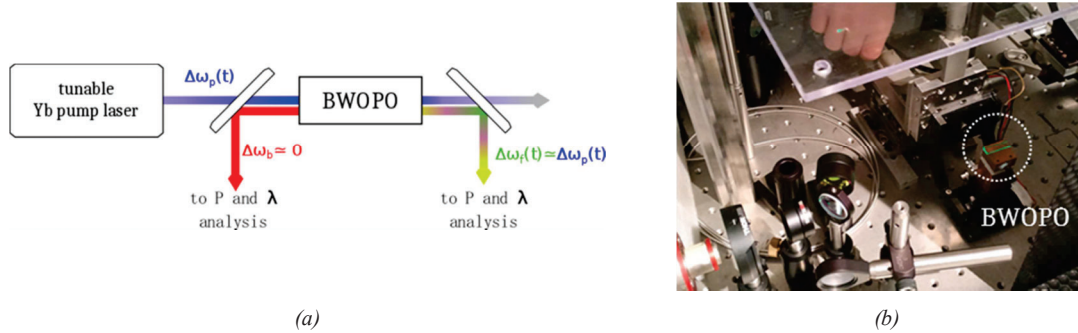


Figure 3: Experimental set-up schematic (a), and laboratory implementation (b) of the BWPO

The pump tuning of the BWPO is consistent with what is theoretically expected from the tuning rates in Table 1. As illustrated in Figure 4, when the pump wavelength is continuously tuned over a 10 GHz span, the BWPO forward frequency follows proportionally with a ratio close to 1, while the backward idler frequency shift (theoretically within a few MHz) remains undetected below the wavemeter resolution. BWPO thus acts as a direct frequency shift translator in the mid-infrared. This is a useful property for remote gas sensing applications such as spaceborne IPDA lidar, where fast ON and OFF absorption line wavelength tuning over several GHz is required. For instance, in the present work our wavelength modulation rate is limited to  $\sim 0.1$  Hz by the measurement integration time on the backward beam wavelength-meter. In a future work spectral characterizations through beat note analysis with an ancillary CW laser would give access to higher sensitivity and speed measurement up to pulse to pulse (at a 5 kHz repetition rate) frequency and linewidth characterizations of the BWPO.

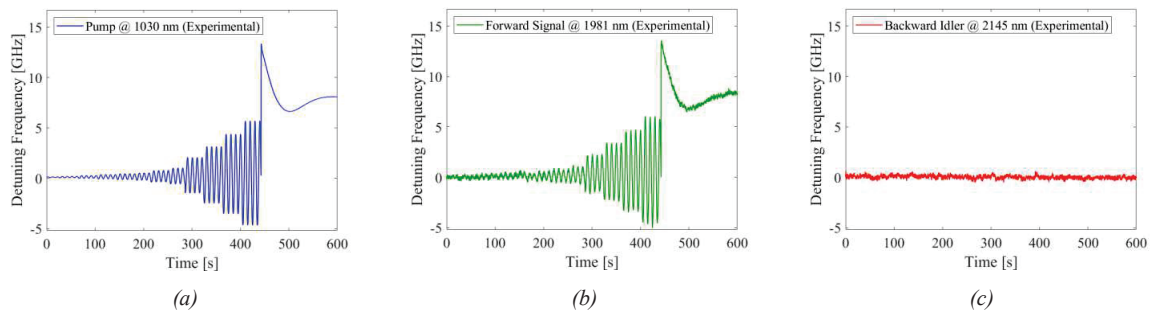


Figure 4: Experimental pump wavelength tuning with a progressive increasing optical frequency excursion over 10 GHz (a), corresponding BWPO frequency tuning for the forward (b) and backward (c) waves.

Finally, Figure 5 gives the output power characteristics for both 7 mm and 17 mm nonlinear crystals. The oscillation threshold is 370  $\mu$ J and 70  $\mu$ J for the short and long crystal respectively, corresponding approximately to 100 MW/cm<sup>2</sup> and 20 MW/cm<sup>2</sup> intensities. The pulse duration of the parametric waves was about 12 ns. In the current experiment up to 0.60 mJ of forward signal wave and 0.36 mJ of backward idler wave could be extracted from the 7 mm crystal and 1.9 mJ of pump energy input. This corresponds to an optical conversion efficiency of approximately 50%. As introduced in part 2.3, the conversion efficiency follows a monotonic trend even for high pumping rates as illustrated in Figure 5(b) in the 17 mm crystal case, where total conversion efficiency reaches  $\sim 70\%$  around 10 times above the threshold. These power and efficiency characteristics are comparable with what may be obtained in high power co-propagating OPOs based on similar nonlinear crystals, but with a much simpler arrangement and very limited detrimental backconversion effects that tend to degrade the beam and spectral quality in conventional OPOs.

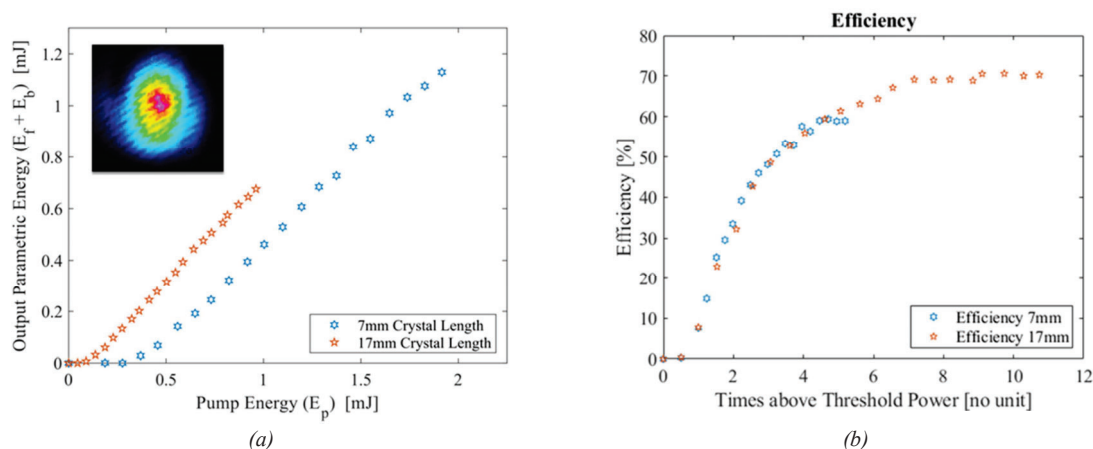


Figure 5: Power characteristics, with the total forward + backward extracted energy from the BWOP respect with pump energy (a), and the corresponding total optical to optical conversion efficiency (b) for two different PPKTP crystal lengths. The inset in (a) is an intensity profile of the 1981 nm forward beam.

#### 4. CONCLUSION

In conclusion we have demonstrated an original BWOP configuration, where the forward signal wave is directly and continuously frequency tuned in the mid-infrared through pump wavelength tuning. This is made possible by using a high power Ytterbium MOPA as the pump source achieving single frequency multi-mJ nanosecond pulses with very high beam quality. Thanks to the progresses in small QPM periodicity developments in the 500 nm – 600 nm range, a tunable forward wave could be generated in the 2  $\mu$ m spectral region suitable for future gas remote sensing applications, including spaceborne CO<sub>2</sub> IPDA lidar. Besides direct pump tuning, this BWOP configuration exhibits attractive characteristics, with accessible oscillation thresholds fluences in the nanosecond regime well below optical induced damaging in PPKTP, high conversion efficiency > 50 % in the mJ energy range with inherently limited backconversion defects, and a compact arrangement with no free-space optical cavities involved. Future research work will concentrate on the spectral quality characterization of the tunable forward wave. Indeed, plane wave theory shows that when pumped with a single frequency laser BWOP naturally emits a Fourier-transform-limited backward and forward wave spectrum<sup>25</sup>. It is thus important to verify how this property deviates in practice due to imperfections in the nonlinear crystal QPM period, in the pump beam propagation, and in the pump beam spectrum itself.

This work has been done under the framework of the LEMON project, EC grant agreement No. 821868, and of the “Investissements d’Avenir” LabEx PALM program (ANR-10-LABX-0039-PALM).

#### REFERENCES

- [1] G. Ehret, C. Kiemle, M. Wirth, A. Amediek, A. Fix, and S. Houweling, "Space-borne remote sensing of CO<sub>2</sub>, CH<sub>4</sub>, and N<sub>2</sub>O by integrated path differential absorption lidar: a sensitivity analysis," *Appl. Phys. B* **90**, 593–608 (2008).
- [2] S. Hahn, M. Bode, J. Luttmann, and D. Hoffmann, "FULAS: high energy laser source for future LIDAR applications," in *International Conference on Space Optics 2018* (SPIE, 2019), Vol. 11180, pp. 1964–1975.
- [3] T. Taira and H. Ishizuki, "Large-Aperture PPMgLN for High Energy Parametric Process," in *Nonlinear Optics (2013), Paper NTu2B.3* (Optica Publishing Group, 2013), p. NTu2B.3.
- [4] R. S. Coetzee, N. Thilmann, A. Zukauskas, C. Canalias, and V. Pasiskevicius, "Nanosecond laser induced damage thresholds in KTiOPO<sub>4</sub> and Rb:KTiOPO<sub>4</sub> at 1  $\mu$ m and 2  $\mu$ m," *Opt. Mater. Express*, *OME* **5**, 2090–2095 (2015).
- [5] A. Zukauskas, N. Thilmann, V. Pasiskevicius, F. Laurell, and C. Canalias, "5 mm thick periodically poled Rb-doped KTP for high energy optical parametric frequency conversion," *Opt. Mater. Express*, *OME* **1**, 201–206 (2011).
- [6] F. Elsen, M. Livrozet, M. Strotkamp, J. Wüppen, B. Jungbluth, R. Kasemann, J. Löhning, A. Meissner, R. Meyer, D. Hoffmann, and R. Poprawe, "Demonstration of a 100 mJ OPO/OPA for future lidar applications and LIDT

- testing of optical components for MERLIN," in *Solid State Lasers XXVI: Technology and Devices* (SPIE, 2017), Vol. 10082, pp. 311–316.
- [7] J. Caron, Y. Durand, J.-L. Bezy, and R. Meynard, "Performance modeling for A-SCOPE: a space-borne lidar measuring atmospheric CO<sub>2</sub>," in *Lidar Technologies, Techniques, and Measurements for Atmospheric Remote Sensing V* (SPIE, 2009), Vol. 7479, pp. 105–119.
- [8] P. Bousquet, C. Pierangelo, C. Bacour, J. Marshall, P. Peylin, P. V. Ayar, G. Ehret, F.-M. Bréon, F. Chevallier, C. Crevoisier, F. Gibert, P. Rairoux, C. Kiemle, R. Armante, C. Bès, V. Cassé, J. Chinaud, O. Chomette, T. Delahaye, D. Edouart, F. Estève, A. Fix, A. Friker, A. Klonecki, M. Wirth, M. Alpers, and B. Millet, "Error Budget of the MEthane Remote Lidar mission and Its Impact on the Uncertainties of the Global Methane Budget," *Journal of Geophysical Research: Atmospheres* **123**, 11,766–11,785 (2018).
- [9] G. Ehret, P. Bousquet, C. Pierangelo, M. Alpers, B. Millet, J. B. Abshire, H. Bovensmann, J. P. Burrows, F. Chevallier, P. Ciais, C. Crevoisier, A. Fix, P. Flamant, C. Frankenberg, F. Gibert, B. Heim, M. Heimann, S. Houweling, H. W. Hubberten, P. Jöckel, K. Law, A. Löw, J. Marshall, A. Agusti-Panareda, S. Payan, C. Prigent, P. Rairoux, T. Sachs, M. Scholze, and M. Wirth, "MERLIN: A French-German Space Lidar Mission Dedicated to Atmospheric Methane," *Remote Sensing* **9**, 1052 (2017).
- [10] A. Fix and C. Stöckl, "Investigations on the beam pointing stability of a pulsed optical parametric oscillator," *Opt. Express*, OE **21**, 10720–10730 (2013).
- [11] J. Hamperl, J. F. Geus, K. M. Mølster, A. Zukauskas, J.-B. Dherbecourt, V. Pasiskevicius, L. Nagy, O. Pitz, D. Fehrenbacher, H. Schaefer, D. Heinecke, M. Strotkamp, S. Rapp, P. Denk, N. Graf, M. Dalin, V. Lebat, R. Santagata, J.-M. Melkonian, A. Godard, M. Raybaut, and C. Flamant, "High Energy Parametric Laser Source and Frequency-Comb-Based Wavelength Reference for CO<sub>2</sub> and Water Vapor DIAL in the 2  $\mu$ m Region: Design and Pre-Development Experimentations," *Atmosphere* **12**, 402 (2021).
- [12] H. Riris, K. Numata, S. Wu, and M. Fahey, "The challenges of measuring methane from space with a LIDAR," *CEAS Space J* **11**, 475–483 (2019).
- [13] M. Livrozet, B. Gronloh, H. Faidel, J. Luttmann, and D. Hoffmann, "Optical and optomechanical design of the MERLIN laser optical bench," in *International Conference on Space Optics — ICSO 2020* (SPIE, 2021), Vol. 11852, pp. 1176–1189.
- [14] P. Mahnke, H. H. Klingenberg, A. Fix, and M. Wirth, "Dependency of injection seeding and spectral purity of a single resonant KTP optical parametric oscillator on the phase matching condition," *Appl. Phys. B* **89**, 1–7 (2007).
- [15] P. Mahnke and M. Wirth, "Real-time quantitative measurement of the mode beating of an injection-seeded optical parametric oscillator," *Appl. Phys. B* **99**, 141–148 (2010).
- [16] A. Fix, C. Büdenbender, M. Wirth, M. Quatrevalet, A. Amediek, C. Kiemle, and G. Ehret, "Optical parametric oscillators and amplifiers for airborne and spaceborne active remote sensing of CO<sub>2</sub> and CH<sub>4</sub>," in *Lidar Technologies, Techniques, and Measurements for Atmospheric Remote Sensing VII* (SPIE, 2011), Vol. 8182, pp. 28–37.
- [17] J. B. Dherbecourt, M. Raybaut, J. M. Melkonian, J. Hamperl, R. Santagata, M. Dalin, V. Lebat, A. Godard, C. Flamant, J. Totems, P. Chazette, V. Pasiskevicius, D. Heinecke, H. Schäfer, M. Strotkamp, J. F. Geus, S. Rapp, H. Sodemann, and H. C. Steen-Larsen, "Design and pre-development of an airborne multi-species differential absorption Lidar system for water vapor and HDO isotope, carbon dioxide, and methane observation," in *International Conference on Space Optics — ICSO 2020* (SPIE, 2021), Vol. 11852, pp. 781–790.
- [18] T. Hamoudi, M. Guionie, X. Delen, J.-B. Dherbecourt, J.-M. Melkonian, A. Godard, M. Raybaut, and P. Georges, "High power, tunable hybrid fiber/bulk laser at 1030 nm and parametric frequency conversion in the near and mid-infrared," *Appl. Phys. B* **128**, 93 (2022).
- [19] S. E. Harris, "Proposed backward wave oscillation in the infrared," *Appl. Phys. Lett.* **9**, 114–116 (1966).
- [20] J. B. Khurgin, "Mirrorless magic," *Nature Photon* **1**, 446–447 (2007).
- [21] Y. J. Ding and J. B. Khurgin, "Backward optical parametric oscillators and amplifiers," *IEEE Journal of Quantum Electronics* **32**, 1574–1582 (1996).
- [22] C. Canalias and V. Pasiskevicius, "Mirrorless optical parametric oscillator," *Nature Photon* **1**, 459–462 (2007).
- [23] R. S. Coetsee, A. Zukauskas, C. Canalias, and V. Pasiskevicius, "Low-threshold, mid-infrared backward-wave parametric oscillator with periodically poled Rb:KTP," *APL Photonics* **3**, 071302 (2018).
- [24] G. Strömqvist, V. Pasiskevicius, and C. Canalias, "Self-established noncollinear oscillation and angular tuning in a quasi-phase-matched mirrorless optical parametric oscillator," *Appl. Phys. Lett.* **98**, 051108 (2011).
- [25] A. Godard, M. Guionie, J.-B. Dherbecourt, J.-M. Melkonian, and M. Raybaut, "Backward optical parametric oscillator threshold and linewidth studies," *J. Opt. Soc. Am. B, JOSAB* **39**, 408–420 (2022).